State-of-Charge Determination in Lithium-Ion Battery Packs Based on Two-Point Measurements in Life

Matthieu Dubarry, Cyril Truchot, Arnaud Devie, and Bor Yann Liaw[*,z]

Hawaii Natural Energy Institute, SOEST, University of Hawaii at Manoa, Honolulu, Hawaii 96822, USA

The state-of-charge (SOC) estimation is of extreme importance for the reliability and safety of battery operation. How to estimate SOC for an assembly of cells in a battery pack remains a subject of great interest. Here a viable method for SOC determination and tracking for multi-cell assemblies is proposed and validated. Using 3S1P (three in series and one in parallel) strings as an example, an inference of SOC is illustrated in a battery assembly based on a correct open pack voltage (OPV) versus SOC (i.e. OPV = f(SOC)) function. The proposed method only requires the measurements of the rest cell voltages of the single cells at two distinct occasions. This accurate SOC estimation approach shall facilitate reliable battery control and management.
 [DOI: 10.1149/2.0201506jes]

Manuscript submitted December 1, 2014; revised manuscript received January 19, 2015. Published March 2, 2015.

Rechargeable lithium-ion batteries (LIB) continue being considered viable choices for mobile power and energy storage applications. Yet, a reliable deployment of LIB in powertrains remains very challenging, primarily due to the requirements for reliable multi-cell assemblies to provide high energy and power. Better capability to characterize battery pack performance, identify aging mechanism, and perform state-of-charge (SOC) estimation is desired to achieve great efficiency.[1,2] In our previous work, we devoted substantial effort to understand the behavior of cells in a pack and the impact of cell variability on pack performance.[3,4] We also reported a diagnostic and prognostic approach to identify and quantify cell-aging mechanisms in the course of cycle aging for a number of cell chemistries.[5–11] To enable these methodologies, the SOC determination is the most vital component among all for accurate operation of the battery management system (BMS).[1] In our latest work,[12] we showed that the most accurate method to obtain the SOC of a battery pack is either by measuring the residual capacity (Q_{res}) against the maximum pack capacity (Q_{max}); i.e. ${}_{pack}SOC = Q_{res}/Q_{max}$, or by measuring the rest pack voltage (RPV) to infer SOC based on a SOC versus open pack voltage (OPV) function; i.e. ${}_{pack}SOC = f^{-1}(OPV)$. Both methods, however, suffer from their inoperability in practical applications, due to (1) in the case of capacity measurements, the uncertainty related to Q_{res} in a duty cycle, (2) the fade in the Q_{max} over lifetime, and (3) in the case of voltage-based measurements, the need for accurate OPV across the full SOC range. Therefore, a simple and practical method for SOC estimation remains very desirable.

For a single cell (SC), the open circuit voltage (OCV) versus SOC function is often preferred for SOC determination because in principle, and at the beginning-of-life (BOL) of the cell, the ${}_{sc}SOC = f^{-1}(OCV)$ function is universal for cells of the same chemistry, disregarding size or geometry.[3] Therefore, this $OCV = f(SOC)$ function only needs to be determined once and for all from a single cell of a specific design. Upon aging, uncertainties to this $OCV = f(SOC)$ function are introduced due to aging-pathway dependence.[6] Such variations could be predicted as a function of duty cycle characteristics using the mechanistic model reported in our prior work.[5]

In battery assemblies, SOC determination is more complicated. This is because all single cells are slightly different and might not act perfectly in sync. Each battery pack, therefore, has a characteristic $OPV = f({}_{pack}SOC)$ function[3,4] and, subsequently, no universal function can be used to describe the chemistry. As the pack ages, this complexity shall increase tremendously because of the likelihood of worsening in the cell balancing due to disparities in aging among the cells.

These issues increase the difficulty in performing accurate SOC determination,[12] since the $OPV = f({}_{pack}SOC)$ function needs periodic calibrations via additional characterization. This is the stumbling block for battery manufacturers or pack integrators to provide a reliable operation of the battery system. Several methods were proposed in the literature to assess the SOC and the state-of-health (SOH) of battery packs,[13–17] but they are all beyond what BMS can handle to date. To overcome this difficulty, here we propose a novel approach that offers a simple solution for BMS implementation while retaining sufficient accuracy for SOC and determination. This approach requires two separate measurements of steady cell voltages for all cells in a pack after a sufficient rest period as well as accurate accounting of the capacity Q between these two measurements. In addition, the two measurements need to be at distinct SOCs with negligible aging in-between.

This method shall enable monitoring and tracking the SOC of the pack as well as each single cell in the pack. The following benefits could be obtained from this simple process:

(1) Individual cell SOC can be monitored accurately in the course of pack operation,
(2) The cell imbalance in the pack can be tracked and quantified,
(3) Cell-level control and monitoring can be enhanced for better reliability and safety,
(4) Logistic requirements and accumulated errors can be minimized.

When coupled with our mechanistic modeling tools,[5] the diagnosis (e.g. SOH, imbalance) and prognosis of pack performance (e.g. remaining useful life, or RUL) shall become feasible. This method also makes estimation techniques such as those based on noise filtering (e.g. Kalman filters) or machine-learning for SOC and SOH estimations functional, since many empirical errors could be minimized.

Principles

The theoretical background behind the proposed method is based on three principles:

(1) The SOC of a single cell can be accurately calculated from a rest cell voltage (RCV) and an universal $OCV = f({}_{SC}SOC)$ function deciphered from low rate cycling on any cell of the same batch.[3,12] This $OCV = f({}_{SC}SOC)$ function varies with aging.[5,7]
(2) The capacity variations within cells of the same batch can be described by a quantity called capacity ration, Qr in mAh SOC^{-1}, which is representative of the amount of active materials in the cell.[3] Depending on the quality of the batch, initial variations of capacity ration among cells can go from less than 0.5% to more than 3%.[3,8]

*Electrochemical Society Active Member.
[z]E-mail: bliaw@hawaii.edu

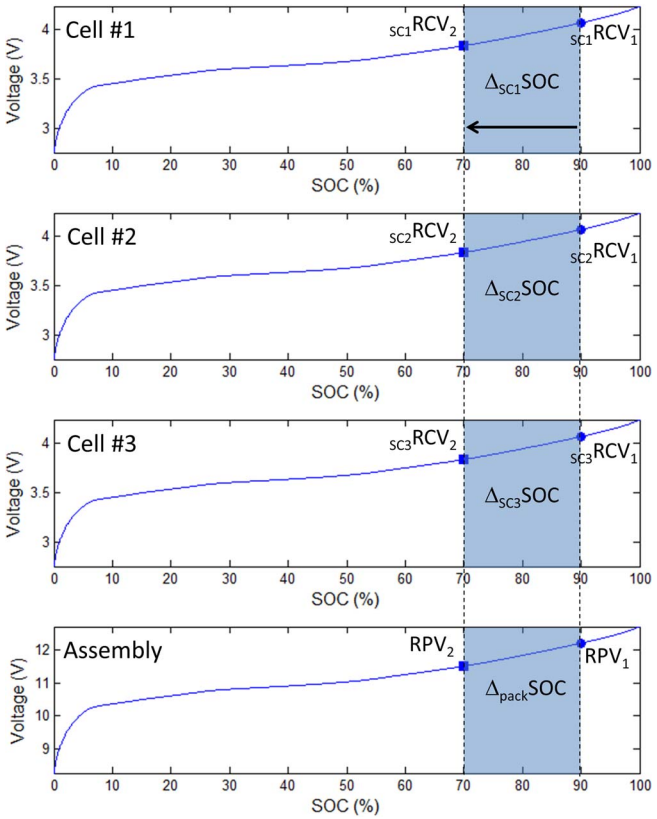

Figure 1. Graphical representation of an ideal and perfectly balanced 3S1P battery pack. The top three panels display the capacity and SOC of the single cells and the bottom panel the cell assembly.

(3) As for the method proposed in our prior work,[5] all $OCV = f(SOC)$ functions can be dissociated mathematically into two independent one-dimensional arrays, *OCV* and *SOC* of the same size. To ease the comprehension of the following sections, arrays will always be noted in italics.

The goal of this approach is to establish a method of inference from the attributes in single cells ($OCV = f(SOC)$ and $_{SC}Qr$) to the attributes in a battery pack ($OPV = f(SOC)$ and $_{pack}Qr$). In order to facilitate the description of this SOC inference method, the following discussions shall focus on four cases with increasing complexity in SOC variations in a hypothetical string of three cells in series (3S1P) of a graphite-Li($Ni_xMn_yCo_z$)O_2 (G||NMC) LIB system. The first case is an ideal battery pack with all single cells having the same capacity ration or $_{SC}Qr$; the same initial SOC or $_{SC}SOC_{ini}$, and the same SOH (i.e. the same $OCV = f(_{SC}SOC)$ function). The second and third cases illustrate how the pack $OPV = f(_{pack}SOC)$ function is influenced by the disparities in $_{SC}SOC_{ini}$ and $_{SC}Qr$, respectively. The fourth case deals with differences in SOHs in the cells (with different $_{SC}OCV = f(_{SC}SOC)$ functions). Through this progressive illustration, we generalize a set of equations to describe the method to determine SOC in any battery assembly.

The $OPV = f(_{pack}SOC)$ simulations were performed using a specific $OCV = f(_{SC}SOC)$ function of a cell chemistry that provided valid test results and a proprietary MATLAB toolbox named *anakonu*[a], established based on the principles developed in this work. The $OCV = f(_{SC}SOC)$ simulations with aging conditions were performed using a proprietary *'alawa*[b][18] toolbox based on the model described in our prior work.[5] Some experimental validation of the *'alawa* simulations for cell aging has been reported by other groups recently.[19,20] The simulations using the *'alawa* model were performed using half-cell data, where the NMC half-cell data was provided by IREQ of Hydro-Quebec, and the data for graphite by TIMCAL.

Ideal battery packs.— Calculating the $OPV = f(_{pack}SOC)$ function of an ideal battery pack, in which all cells are identical (i.e. the same $_{SC}Qr$ and SOH) and in balance (i.e. the same $_{SC}SOC_{ini}$), is straightforward. Since all cells share the same *OCV* and *SOC* arrays, the $OPV = f(_{pack}SOC)$ function is the summation of the $OCV = f(_{SC}SOC)$ functions by the number of cells in the series. The pack cutoff voltages are also in proportion with the number of cells, while the $_{pack}SOC$ and $_{pack}Qr$ are the same as those of the single cells. Figure 1 presents a graphical illustration of a 3S1P pack with three plots showing the individual $OCV = f(_{SC}SOC)$ functions for each of the three cells in the pack and the bottom one the $OPV = f(_{pack}SOC)$ of the pack in this case study.

A set of equations is established to characterize the three attributes related to the pack (*OPV* and $_{pack}SOC$ array and $_{pack}Qr$) as a function of the SC attributes. For visualization of this process, markers were provided in Figure 1 for discussion. The circles ($_{SCi}RCV_1$) correspond to the RCVs measured at $_{SCi}SOC_{ini}$ for cell #*i* in an *n*-cell pack. The squares ($_{SCi}RCV_2$) represent the RCVs after a certain period of discharge with a capacity Q. The shaded area on each curve represents the variation of SOC (ΔSOC) associated with the discharge of capacity Q.

The *OPV* array was calculated based on Kirchhoff's law. Since the cells are connected in series, the rest pack voltages RPV_1 and RPV_2 are calculated as:

$$RPV_j = \sum_{i=1}^{n} {}_{SCi}RCV_j$$

$$(\text{for } j = 1,\ 2;\ \text{and } n = \text{number of cells in the string}) \quad [1]$$

From this equation, the RCVs could be expressed as a function of SOC in each single cell, as inferred by the *OCV* array, if sufficient rest time has been allowed to reach pseudo-equilibrium. Eq. 1 is then expressed as:

$$RPV_j = \sum_{i=1}^{n} {}_{SCi}OCV(_{SCi}SOC_{RCVj}) \quad [2]$$

To calculate the *OPV* array, Eq. 2 should be expressed as a function of a common *SOC* array to allow arithmetic operations. Under this scenario, since all $_{SC}SOC_{ini}$ are the same, all RCV_1 are equal. Since $_{SC}Qr$ is constant, the capacity Q should correspond to the same $\Delta_{SC}SOC$ for all the cells. Furthermore, since the cells are at the same SOH, all RCV_2s should be equal as well. This is true for the entire SOC range and as a result all $_{SCi}SOC$ arrays are identical. Eq. 2 can then be modified to include a common *SOC* array, arbitrarily chosen to be $_{SC1}SOC$, and the *OPV* array can be introduced as:

$$RPV_j = OPV\left(_{SC1}SOC_{RCVj}\right) = \sum_{i=1}^{n} OCV(_{SC1}SOC_{RCVj}) \quad [3]$$

Since Eq. 3 is true for the entire SOC range, it can be generalized to calculate the entire *OPV* array as a function of $_{SC1}SOC$:

$$OPV\,(_{SC1}SOC) = \sum_{i=1}^{n} OCV\,(_{SC1}SOC\,) \quad [4]$$

SC1 was chosen for convenience. To determine the $_{pack}SOC$, following Eq. 4, we continue to use SC1 to express $_{pack}SOC$ as a function of $_{SC1}SOC$ by introducing the pack cutoff voltages OPV_{min} and OPV_{max}. Since the $_{pack}SOC$ should correspond to the maximum capacity the pack could deliver in the operating voltage range,[12] conforming to 100% at OPV_{max} and 0% at OPV_{min}, $_{pack}SOC$ can be calculated by:

$$_{pack}SOC = \frac{_{SC1}SOC - {}_{SC1}SOC(OPV_{min})}{_{SC1}SOC(OPV_{max}) - {}_{SC1}SOC(OPV_{min})}100\% \quad [5]$$

Regarding $_{pack}Qr$, since the cells are in series, the capacity Q discharged is the same for all cells and the pack. Thus, Q can be expressed

[a] *anakonu* is the Hawaiian word for "equilibrium."
[b] *'alawa* is the Hawaiian word for "to diagnose."

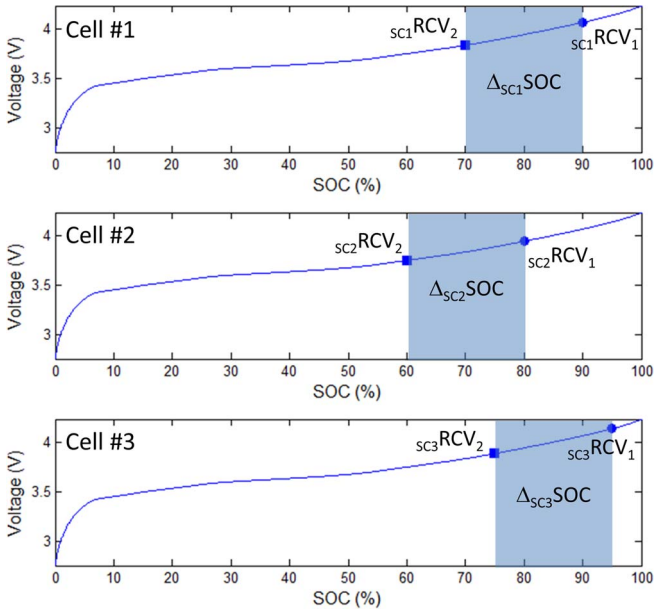

Figure 2. Graphical representation of the single cells in a 3S1P battery pack with different initial SOCs.

as a function of each individual ΔSOC and Qr:

$$Q = \Delta_{SCi}SOC\ {}_{SCi}Qr = \Delta_{pack}SOC_{pack}Qr \quad [6]$$

Eq. 6 can then be rearranged to express ${}_{pack}Qr$:

$${}_{pack}Qr = \frac{\Delta_{SCi}SOC_{SCi}Qr}{\Delta_{pack}SOC} = \frac{Q}{\Delta_{pack}SOC} \quad [7]$$

Using Eqs. 4–7, the pack attributes were successfully expressed as a function of the single cell attributes for this ideal case. In the following scenarios, we shall progressively amend this set of equations to accommodate more complicated cases.

Battery packs with identical cells but different initial SOCs.— Figure 2 presents a case where the cells have different initial SOCs, ${}_{SCi}SOC_{ini}$. Because of the mismatch of initial SOCs, the cells shall have different ${}_{SCi}RCVs$ (as shown by the circles and squares in Figure 2) before and after the discharge. In this case, even if the cells share identical ${}_{SCi}Qr$ and identical *OCV* and *SOC* arrays, Eq. 4 is no longer valid. A simple summation of the three *OCV* arrays cannot be used anymore to calculate the $OPV = f(_{SC1}SOC)$ function because $\Delta_{SC1}SOC$ and other $\Delta_{SCi}SOCs$ are not aligned anymore, as illustrated in Figure 2.

Despite this misalignment, ${}_{sc}Qr$ remains identical and $\Delta_{SC}SOC$ is still the same for all cells. The misalignment can be addressed by a proper translation among the *SOC* arrays. By aligning the $\Delta_{SC}SOC$ ranges properly, the $OCV = f(_{SCi}SOC)$ functions can be translated in order to follow the alignment, as shown in Figure 3. Keeping SC1 as a reference, a translation factor ${}_{SCi}tf$ for $_{SCi}SOC$ versus $_{SC1}SOC$ can be defined as the difference between the SOC at RCV_1 for SC1 and SCi (i = 2, 3):

$${}_{SCi}tf = {}_{SC1}SOC(RCV_1) - {}_{SCi}SOC(RCV_1) \quad [8]$$

The pack $OPV = f(_{SC1}SOC)$ function can be expressed by summing the individual *OCV* arrays after translation as follows:

$$OPV\,(_{SC1}SOC) = OCV\,(_{SC1}SOC) + \sum_{i=2}^{n} OCV\,(_{SC1}SOC + {}_{SCi}tf\,) \quad [9]$$

This modification is able to accommodate SOC imbalance in the pack. Eqs. 5 and 6 remain the same for $\Delta_{pack}SOC$ and ${}_{pack}Qr$.

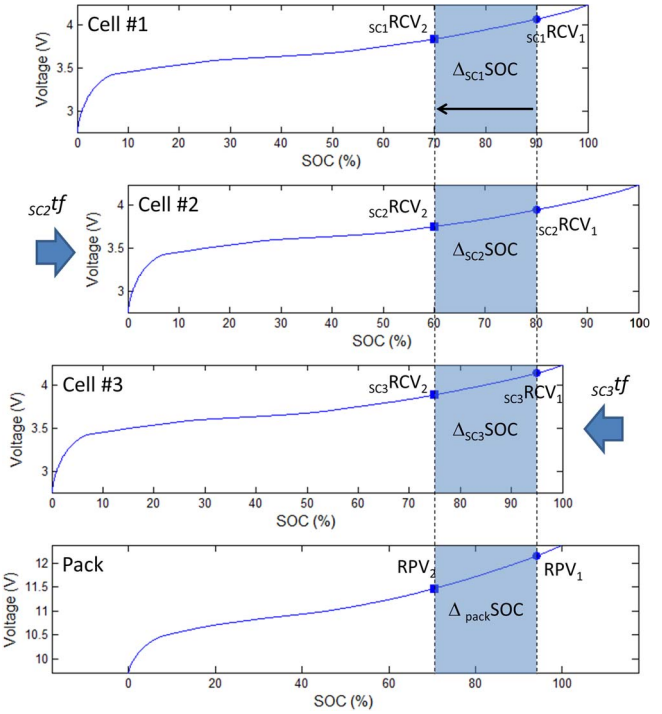

Figure 3. Graphical representation of a 3S1P battery pack after accommodating identical single cells with different initial SOCs. The top three panels display the capacity and SOC of the single cells and the bottom panel the cell assembly.

Battery packs of different capacity rations among the cells.— Figure 4 presents the case where the cells have different capacity rations but identical initial SOC and SOH. In this case, although ${}_{SCi}RCV_1s$ (circles) are the same, ${}_{SCi}RCV_2s$ (squares) are different since cells with different capacity rations shall experience different ΔSOCs for the same capacity Q discharged (see Eq. 6). In this scenario, Eq. 9 becomes inadequate and a simple translation of the *SOC* arrays is not sufficient to express the $_{SCi}SOC$ in each cell. In other words, a simple

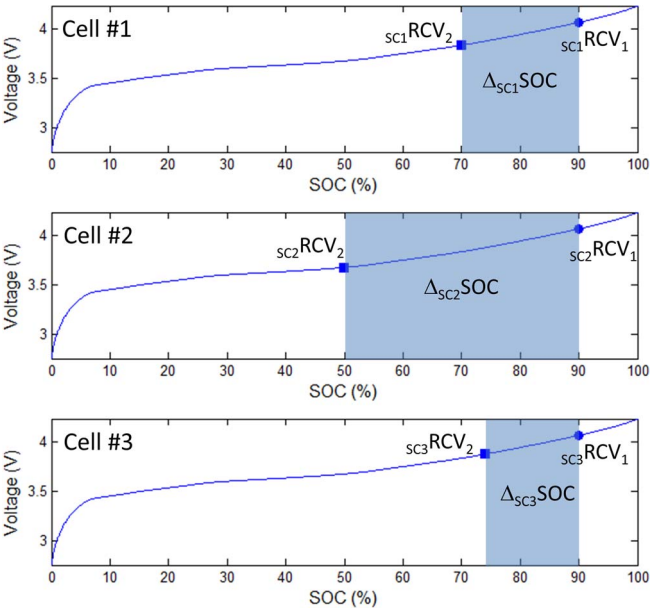

Figure 4. Graphical representation of the single cells in a 3S1P battery pack with different capacity rations.

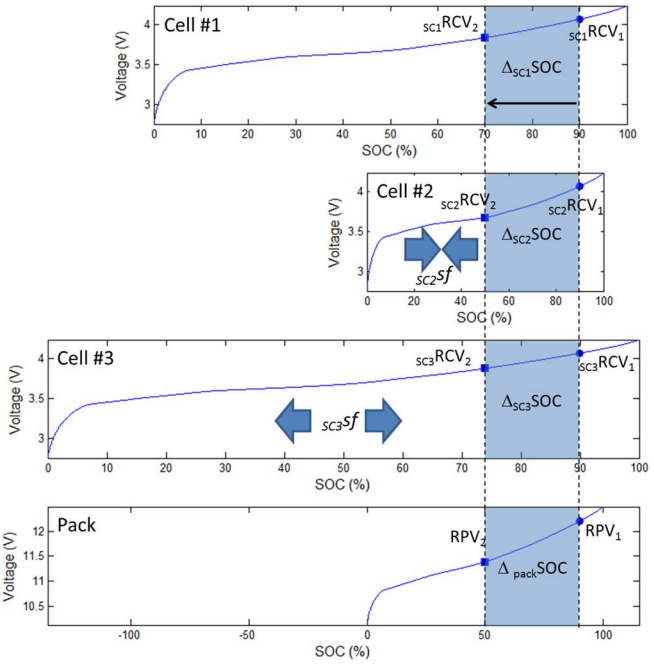

Figure 5. Graphical representation of a 3S1P battery pack after accommodating different capacity rations in single cells having the same initial SOC. The top three panels display the capacity and SOC of the single cells and the bottom panel the cell assembly.

translation is not sufficient to align the $\Delta_{SC}SOC$ properly and additional scaling factors of the *SOC* arrays become necessary, as shown in Figure 5. The introduction of the scaling factors modifies Eq. 9 as follows:

$$OPV\,(_{SC1}SOC) = OCV\,(_{SC1}SOC) + \sum_{i=2}^{n} OCV\,(_{SCi}sf\,(_{SC1}SOC + {}_{SCi}tf)) \quad [10]$$

In this equation, $_{SCi}sf$ is introduced as a scaling factor. This factor can be defined either from the ratio of $_{SCi}Qr$ or from $\Delta_{SCi}SOC$ between two distinct RCVs (cf. Eq. 6):

$$_{SCi}sf = \frac{_{SCi}Qr}{_{SC1}Qr} = \frac{\Delta_{SCi}SOC}{\Delta_{SC1}SOC} = \frac{_{SCi}SOC(RCV_1) - {}_{SCi}SOC(RCV_2)}{_{SC1}SOC(RCV_1) - {}_{SC1}SOC(RCV_2)} \quad [11]$$

These two additional equations show that, if the cells have the same SOH, measuring the RCVs of all single cells at only two distinct occasions shall give sufficient information to calculate the $OPV = f(_{pack}SOC)$ function without the demand to consider imbalance and cell variability in the pack. This is a very significant aspect of this work, implying that a simple $_{pack}SOC$ determination can be achieved by two RCV measurements in the cells at the same temperature, even with imbalance due to different SOCs, as long as the aging is insignificant. More interestingly, if the Qr's are known for the cells, only one RCV measurement is sufficient. With Eqs. 9–11, any imbalance in a pack at BOL should not interfere the $_{pack}SOC$ determination; thus, any additional SOC calibration for a battery pack becomes unnecessary.

Battery packs with cells at different states of health.— In light of the previous results, it is possible to determine $OPV = f(_{pack}SOC)$ and $_{pack}Qr$ at BOL from the single cells, if two sets of RCVs and their original $OCV = f(_{SCi}SOC)$ functions are known. Unfortunately, $OCV = f(SOC)$ functions may change with SOH[5,7] and the degradation is often path dependent, which implies that not all the cells in the pack may age to the same extent. Thus, aged cells could have different capacity rations, $_{SCi}Qr$'s, and $_{SCi}OCV = f(_{SCi}SOC)$ functions.

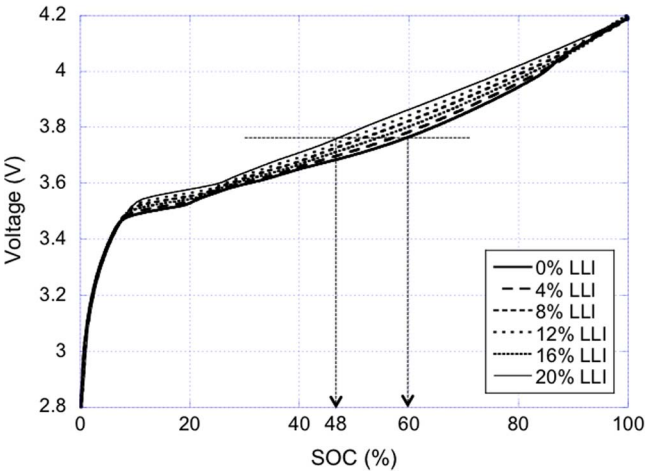

Figure 6. Evolution of the $_{SCi}OCV = f(_{SCi}SOC)$ from the beginning of life to 20% loss of lithium inventory with 4% increments.

As explained before, the variation of capacity ration is not an issue and it can be addressed with a scaling factor sf. To address different $_{SCi}OCV = f(_{SCi}SOC)$ functions, Eq. 10 needs to be modified to accommodate path dependence in the degradation by considering a specific *OCV* array for each single cell, $_{SCi}OCV$, instead of the common $_{SC}OCV$ used previously:

$$OPV\,(_{SC1}SOC) = {}_{SC1}OCV\,(_{SC1}SOC) + \sum_{i=2}^{n} {}_{SCi}OCV\,(_{SCi}sf\,(_{SC1}SOC + {}_{SCi}tf)) \quad [12]$$

Eqs. 5–11 remain the same.

Eq. 12 suggests that if cells were tested individually under different conditions, the acquired knowledge could be used to generate an $OPV = f(_{pack}SOC)$ function to accommodate the cells that might experience different extents of degradation, due to temperature or rate variations. Therefore, coupling this approach with the *'alawa* toolbox[18] opens a possibility for pack diagnosis and prognosis, since the model behind *'alawa* allows simulation of $_{SCi}OCV = f(_{SCi}SOC)$ functions under a wide range of degradation conditions and resulting fades.[5]

An example is illustrated below to highlight the significance of this unique aspect. Calendar aging is known to introduce loss of lithium inventory (LLI),[19,21] and the *'alawa* toolbox could be used to simulate various degrees of LLI in single cells.[5] Based on the *'alawa* simulations, an example of $_{SCi}OCV = f(_{SCi}SOC)$ variations for a G||NMC cell that has undergone up to 20% LLI is shown in Figure 6. The $_{SCi}OCV = f(_{SCi}SOC)$ functions change with LLI degradation at all SOCs above 10%. If not taken into account properly, such variations by aging could compromise the accuracy of SOC estimation. For example, for a RCV measured at 3.75 V, the corresponding SOC could vary from 60% without LLI to 48% at 20% LLI, implying 12% difference in SOC estimation.

The $_{SCi}OCV = f(_{SCi}SOC)$ functions estimated from the *'alawa* toolbox[18] could be fed into the *anakonu* model. Thus, if the degradation associated with a path were known, the accuracy of the $OPV = f(_{pack}SOC)$ could be retained. Figure 7 presents the result of a simulation in which the $OPV = f(_{pack}SOC)$ function for cells having the same RCV_1s but experiencing various degrees of calendar aging, e.g. 0, 10, and 20% LLI, respectively. Figure 7a presents the discharge curves before proper alignment and scaling, and Figure 7b after. In Figure 7a, although the RCV_1s are the same in the single cells (as expected with a conventional balancing circuit at the end of charge), the $_{SC}SOC_{ini}$s are different at 90%, 88% and 86% from SC1 to SC3, respectively. For better comparison, the dashed lines show the initial OCV versus SOC curves. After proper alignment and scaling,

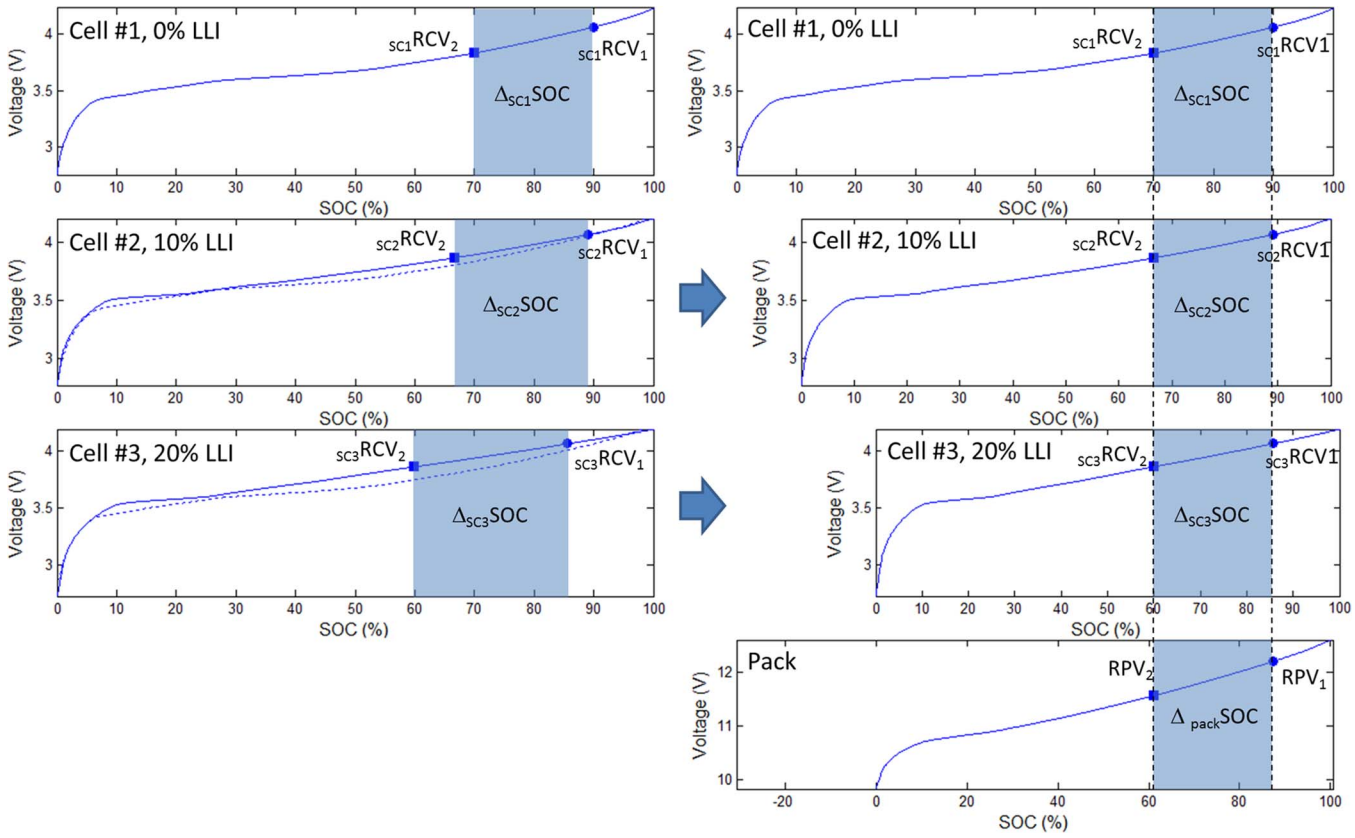

Figure 7. Graphical representation of a 3S1P battery pack (a) before and (b) after accommodating different SOH in single cells. The top three panels display the capacity and SOC of the single cells and the bottom panel the cell assembly. The dashed lines display the original OCV versus SOC curves for Cells #2 and #3.

Figure 7b shows that the $\Delta_{SC}SOC$ ranges were aligned. The change in the sf value corresponds to the specific loss of capacity associated with LLI in each cell. Overall, the pack capacity is predicted to be about 23% smaller than that of a pack with pristine cells.

In summary, the *anakonu* model is simple and easy for implementation in BMS since voltage measurements on single cells can be made readily available. The $_{SCi}OCV = f(_{SCi}SOC)$ functions can be stored as lookup tables. Stable RCVs could be obtained usually after three to four hours of rest. To shorten the duration of yielding stable RCVs, one can exercise numerical curve fitting, estimation by approximations, or filtering techniques to estimate the final values with sufficient accuracy. The *'alawa* toolbox[18] also requires very little computation power. Although the examples presented here are with 3S1P strings, this approach could be easily scaled up for more complicated pack configurations with a large number of cells in series and parallel. Even though parallel operation was not illustrated here, it would be discussed elsewhere.[22] In addition, this method may also show merits to define metrics and quantify reliability for a battery pack in the presence of imbalance and its subsequent impacts on pack operation with aging. The evolutions of the tf, sf and Qr for each cell and pack upon aging could be monitored, quantified and used for prognosis of RUL. Ultimately, sf and tf could be used to design and implement more intelligent balancing protocols to maximize battery pack performance, enable realistic life prediction, and provide adequate safety monitoring.

Experimental

To validate the proposed *anakonu* method, two types of commercial LIB cells obtained from E-One Moli Energy Corp. (Molicel) were evaluated in this study. The first type is Molicel IHR 18650A, which comprised graphite negative electrode and $LiNi_{1/3}Mn_{1/3}Co_{1/3}O_2$ (NMC) positive electrode. The second type is 1.4 Ah Molicel IMR 18650E with graphite negative electrode and $LiMn_2O_4$ (LMO) positive. A nominal sample cell from each type was used in C/25 charge and discharge regimes to determine the initial $OCV = f(_{SC}SOC)$ functions.[3]

3S1P strings made of three cells of the same type were assembled for experiments, and data was collected to derive relevant information for validation of the *anakonu* principles. To further illustrate the concept, experiments with different operating conditions were set up and imbalance among the cells was introduced intentionally to verify the accuracy of the SOC estimations. Two sets of experiments were performed as follows:

(1) A 3S1P string of three G||NMC cells with one cell deliberately charged to 90% SOC and the other two to 100% SOC initially was tested to study the case of pack imbalance. Following the same methodology as described in Ref. 12, a C/25 charge discharge cycle was performed initially to determine the $OPV = f(_{pack}SOC)$ function of this specific string. Additional charge-discharge cycles have been conducted at C/2, 1C, 2C and 2.5C, respectively. More details on the testing procedure of the G||NMC IHR18650A cell are in Ref. 12. The cutoff voltages for the charge and discharge regimes were 12.6 V and 9.4 V, respectively. The rest period was four hours between two consecutive regimes. The same procedure was applied here to collect data for analysis and for the understanding of the pack imbalance.

(2) A 3S1P G||LMO string with no SOC imbalance among the cells at BOL and 25°C, but with one cell constantly exposing to 60°C during cycle aging, was used to study the influence of thermal imbalance. The string was cycled for 200 cycles at 2C using protocols derived from the specifications provided by the cell manufacturer, including recommended cutoffs and charging conditions. A C/25 full charge discharge cycle was performed every 30

cycles to characterize the degree of aging, as part of a reference performance test (RPT) that comprises full charge-discharge cycles at C/25, C/2 and 5C. The cutoff voltages used in the cycle were of 12.6 V and 9 V, respectively, in the charge and discharge regime, for the string. The rest period was four hours between two consecutive regimes. In parallel, two single cells were cycle aged at 2C respectively at 25°C and 60°C using the same cutoffs (4.2 V and 3.0 V, respectively, per cell) and charging conditions. The rest period was also four hours between consecutive test regimes. The same RPT was also performed on these cells for comparison. Details of this G||LMO study are out of the scope of this paper and will be published elsewhere.[23]

Results and Discussion

Case study (1) – situation with cell imbalance.— In our previous work[12] a 3S1P G||NMC pack has been extensively tested at C/5, C/2, 1C, 2C and 2.5C to derive the most effective method to determine the SOC of the pack experimentally. In that investigation, the $OPV = f(_{pack}SOC)$ and $_{pack}$Qr were determined experimentally. Using the RPVs at the beginning and end of any of the discharge or charge regimes, the simulated $OPV = f(_{pack}SOC)$ curve could be derived by the *anakonu* method and used for validation. The curve of the initial state is shown in Figure 8, in which the circles represent the experimental data obtained in the prior work[12] and the solid line the reconstructed function using the initial and final RCVs from the C/2 discharge regime of the same experiment and the *anakonu* method. The C/2 rate was chosen arbitrarily. Results of other rates were found to be similar. The mean error in the voltage between the two $OPV = f(_{pack}SOC)$ curves is 3.5 mV, which is about the same as the tester's voltage resolution, ±3 mV.[12] The maximum error is 8.5 mV near 45% SOC. The error in the SOC estimation between the one inferred from the OPVs estimated by the *anakonu* method and the one from that reported in Ref. 12 is on average ±0.2% and the most 0.55%. This is comparable to the error that might have been introduced by the tester's voltage resolution. In contrast, deriving the $OPV = f(_{pack}SOC)$ function by using techniques other than the RCV method would have led to errors on the order of 3% on average (c.f. the $^{Avg(OCV)}_{string}SOC$ method in Ref. 12, which came with an upper and lower bound from +7% to –3% in error).

In short, the *anakonu* method is very effective in deriving the $OPV = f(_{pack}SOC)$ function for a battery pack. The method comprises a one-time determination of the $OCV = f(_{SC}SOC)$ function on a sample cell and on two distinct occasions the RPVs of all the cells in the pack during operation. Based on this method, in the case illustrated, the calculated capacity ration $_{pack}$Qr is 18.65 mAh SOC^{-1}, which suggests the capacity of the pack is 1.865 Ah, close to the 1.845 Ah measured at C/25, as reported in Ref. 12. This verification indicates that this *anakonu* method provides an accurate account of SOC imbalance in the cells introduced in this case study before cycle aging. It can produce $OPV = f(_{pack}SOC)$ function and $_{pack}$Qr for a battery pack accurately and reliably even with significant imbalance. It can be used as a pack design tool to assess the capacity influenced by the degree of imbalance. As cells age, while the cell imbalance in the pack could increase, it can be used as a diagnostic and prognostic tool to analyze the SOC variations with aging conditions.

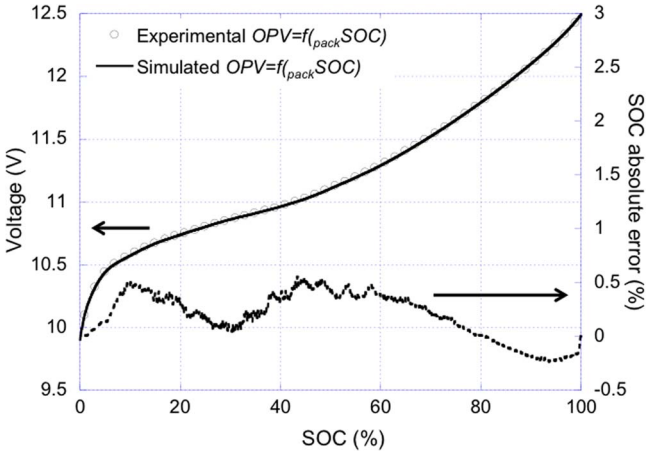

Figure 8. Comparison of experimental and simulated $OPV = f(_{pack}SOC)$ function for a 3S1P G||NMC string with 10% SOC imbalance.

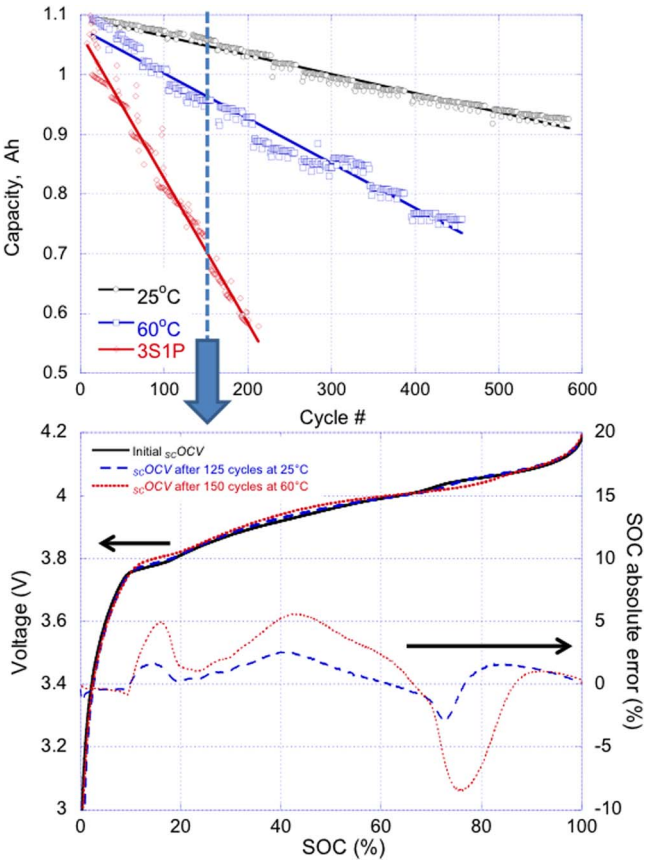

Figure 9. (a) Capacity variation under 2C cycle aging for G||LMO single cells at 25°C (black ○), 60°C (blue □) and a 3S1P string with 2 cells at 25°C and 1 cell at 60°C (red ◊). (b) Corresponding $_{SCi}OCV = f(_{SCi}SOC)$ and $OPV = f(_{pack}SOC)$ after 150 cycles of aging, where the difference from the initial one is shown on the right scale.

Case study (2) – situation with path dependence in aging.— Figure 9a presents the capacity fading results for the single cells and the pack for the second case study with the G||LMO string. The capacity fade is more severe at 60°C than at 25°C for the cells. The capacity fade of the pack is three times higher than that of the cell at 60°C and six times higher than that of the cell at 25°C. The degradation mechanism responsible for these fades shall be discussed elsewhere.[23] Here, the results and verification of the SOC estimates by the *anakonu* method are discussed. A key question is to address the higher capacity fade in the pack than those in the cells. Is it a result of (initial) intrinsic imbalance among the cells or the extrinsic imbalance introduced by operation conditions and escalated during aging? In other words, is it possible to separate the contributions intrinsically due to initial cell variability from those due to the evolution of cell imbalance in the pack in the course of aging?

By examining the experimental $_{SCi}OCV = f(_{SCi}SOC)$ and $OPV = f(_{pack}SOC)$ functions, we could determine the variations in the SOCs at different SOHs using the *anakonu* method. Figure 9b shows the comparison among the BOL $_{SCi}OCV = f(_{SCi}SOC)$ function and

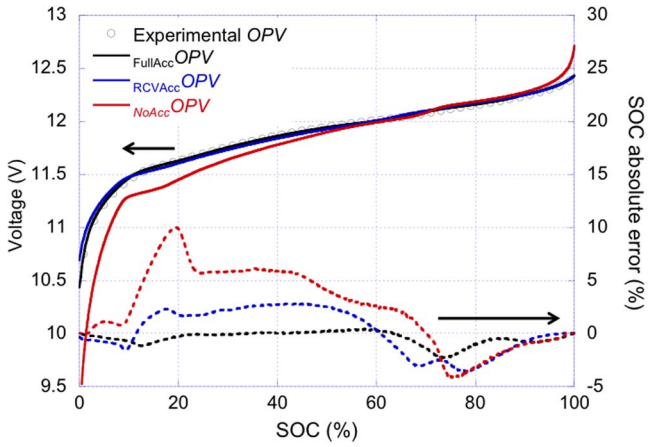

Figure 10. Comparison of experimental and simulated $OPV = f(_{pack}SOC)$ functions for a 3S1P G||LMO string with a temperature gradient. Simulations were performed for three scenarios: (1) no accommodation of cell variability, (2) accommodating RCV variations only, and (3) a full accommodation of RCV and SOH variations.

those received later by cycle aging for the single cells. The $_{SCi}OCV = f(_{SCi}SOC)$ function of the cell aged at 25°C for 125 cycles is fairly close to the initial one, but some subtle differences in the SOC estimation are not negligible, about 1.1% on average, with an upper and lower bound from 3% to –3%. The errors are most noticeable in the vicinity of 15%, 42% and 75% SOC. The $_{SCi}OCV = f(_{SCi}SOC)$ function of the cell aged at 60°C for 150 cycles reveals more disparities, on average 2.82%, with an upper and lower bound in error from 6% to –8.5%. The capacity ration of the cells at the BOL was about 11.4 mAh SOC^{-1}, whereas it was 10.6 and 9.5 mAh SOC^{-1} after aging at 25°C and 60°C, respectively.

Applying Eqs. 4, 10, and 12, $OPV = f(_{pack}SOC)$ and $_{pack}$QR estimations could be derived from these $_{SCi}OCV = f(_{SCi}SOC)$ functions. Three scenarios of $OPV = f(_{pack}SOC)$ variations were investigated here. The first one is a scenario with an ideal pack, using Eq. 4 with the original $OCV = f(_{SCi}SOC)$ function and $_{SC}$Qr without considering any imbalance. Since there is no RCV accommodation, this scenario was dubbed 'NoAcc'. This scenario corresponds to how a typical BMS works today, disregarding aging, any temperature gradient, or imbalance. In the second scenario (dubbed 'RCVAcc'), the effect of imbalance and its evolution in the changes of the RCVs is considered, as exemplified in Eq. 10. The third scenario (dubbed 'FullAcc') uses Eq. 12 to accommodate both imbalance and variations in $_{SC}Qr$ and $_{SCi}OCV = f(_{SCi}SOC)$ functions. The RCVs used in the calculations were gathered from cycle 140, which was a 2C discharge, and they were 4.121 V and 3.858 V for Cell #1, 4.093 V and 3.765 V for Cell #2, and 4.140 V and 3.873 V for Cell #3. The measured capacity Q was 0.734 Ah.

Figure 10 presents the three $OPV = f(_{pack}SOC)$ simulations compared to the experimental data. The errors in the SOC estimation for each case are provided (dotted curves) in the figure. The error is the difference between the calculated SOCs and the experimental ones. The $_{NoAcc}OPV$ (in red) was calculated without any accommodation of the SOC variations among the cells, and the result was the worst, most noticeably in the low and high SOC ranges. On average, the error was 3.7% with upper and lower bounds at 10% and –5%, respectively. The $_{RCVAcc}OPV$ (in blue) was calculated with accommodation of initial SOC variations among the cells. The result was much better with an average of 1.8% in error and an upper and lower bound at 3% and –3% respectively. The $_{FullAcc}OPV$ (in black) came with full accommodation of SOC variations through aging and was by far the most accurate result with only 0.5% error on average and an upper and lower bound at 0.5% and –2.5%, respectively. It should be noted that the largest error in SOC estimates were found in the vicinity of 12% and 73% SOC, where impacts from cycle aging were the most (Figure 9b).

Table I. Calculated $_{pack}Qr$ vs. experimental result and the error assessed.

	Estimated $_{pack}$Qr (mAh SOC^{-1})	Error (%)
$_{pack}Qr^{Exp}$	8.52	
$_{pack}Qr^{FullAcc}$, Q /ΔSOC method	8.53	0.04%
$_{pack}Qr^{RCVAcc}$, Q /ΔSOC method	8.58	0.63%
$_{pack}Qr^{FullAcc}$, $_{SC}$Qr Δ_{SC}SOC /ΔSOC method	8.65	1.69%
$_{pack}Qr^{RCVAcc}$, $_{SC}$Qr Δ_{SC}SOC /ΔSOC method	9.59	11.11%
$_{pack}Qr^{NoAcc}$	11.40	25.24%

The *anakonu* approach has been illustrated for its capability in accommodating cell variations in SOC in a pack due to intrinsic imbalance and the effect of aging path dependence. Better than 0.5% in SOC determination on average after 33% capacity loss in the pack is achievable. One should be reminded that the quality of the data depends on the resolution and accuracy of the measuring devices and that an accurate voltage measurement is a prerequisite for a precise SOC estimation based on the $OPV = f(_{pack}SOC)$ function.

A precise SOC determination does not guarantee an accurate SOC tracking. Indeed, even if SOC is calibrated often, its changes (on an absolute scale where thermodynamics reigns) cannot be computed dynamically with this method. Dynamic SOC tracking could be performed using coulomb counting where the Δ_{pack}SOC is calculated by an integration of the current. An accurate account of the capacity vs. SOC relationship is therefore necessary. The changes in the capacity ration could be an effective approach to assist SOC tracking with aging. According to Eq. 7, there are two methods to calculate $_{pack}$Qr from the Δ_{pack}SOC: The first method is to divide the experimental capacity Q by the calculated Δ_{pack}SOC. The second one is to divide the (Δ_{sc}SOC × $_{SC}$Qr) by the Δ_{pack}SOC for each single cell. Therefore, the *anakonu* method can also be used to assist SOC tracking.

In order to exemplify the utility of the *anakonu* method for SOC tracking, the simulation presented in Figure 10 was used to calculate the $_{pack}$Qr and compare with the experimental one. The results for the three scenarios, NoAcc, RCVAcc, and FullAcc; by the two $_{pack}$Qr calculation methods are compiled in Table I for comparison. As anticipated, the worst $_{pack}$Qr estimation was the one obtained from the simulation without any accommodation (NoAcc), where the $_{pack}$Qr was the same as the fresh cell, 11.4 mAh SOC^{-1}, 25% higher than the experimental value, $_{pack}Qr^{Exp}$, of 8.52 mAh SOC^{-1}. When $_{pack}$Qr was estimated from the Q/Δ_{pack}SOC method, both RCVAcc and FullAcc treatments provide an estimate at 8.53 and 8.58 mAh SOC^{-1}, respectively. The $_{pack}Qr^{RCVAcc}$ was 0.6% off the experimental one, whereas the $_{pack}Qr^{FullAcc}$ was nearly identical (i.e. 0.04% off). When the $_{pack}$Qr was estimated from the Δ_{pack}SOC/(Δ_{sc}SOC × $_{SC}$Qr) method, there was a noticeable disparity between the simulations of the FullAcc and RCVAcc treatments. The $_{pack}Qr^{FullAcc}$ was calculated to be 8.65 mAh SOC^{-1}, 1.7% off the experimental data, whereas the $_{pack}Qr^{RCVAcc}$ was calculated to be 9.59 mAh SOC^{-1}, 11% off. This was expected since the $_{SC}$Qr values should vary with aging, depending on the aging mechanism; thus, the calculation with the initial $_{SC}$Qr was not expected to give an accurate account in the RCVAcc calculation. Regarding the $_{pack}Qr^{FullAcc}$, the error is slightly larger than what we expected. By comparing the $_{SC}$Qr from cell to cell, it seems that the cells at 25°C were accurate at 8.53 mAh SOC^{-1} on average; but, the cell at 60°C gave an $_{SC}$Qr at 8.94 mAh SOC^{-1}, 4.5% off the experimental value. This difference could be due to the fact cells do not aged at exactly the same pace even when cycled in identical conditions.[24] Cell #2 might have then aged a little faster than of the reference cell at 60°C. In conclusion, the $_{pack}$Qr values could be accurately calculated if the capacity between the two RCVs were known. If it is not accurately measured, accuracy could be compromised; however, in general, the $_{pack}$Qr could be calculated from the single cells with good faith

estimation if a full accommodation of the cell imbalance has been performed in the estimate process.

Another interesting aspect in the analysis of the simulation results presented in Figure 10 is the evolution of the $_{sc}$tf and $_{sc}$sf coefficients with aging. With the FullAcc approach, the evolution of the cell imbalance in the pack with aging could be evaluated. The $_{sc}$sfs varied from 1.018 and 0.999, initially, to 0.865 and 1.000 after aging in Cell #2 and #3, respectively, as compared to Cell #1. The $_{sc}$sf remains close to 1 for Cell #3, which implies that both Cell #1 and #3 faded in the same way. This was expected, since they were cycle aged under the same condition. The $_{sc}$sf in Cell #2 decreased from 1.018 to 0.865, suggesting that it faded more severely with 86.5% of the capacity retained in Cell #1 available after 150 cycles. As shown in Figure 9a, the capacity of the cell cycled at 60°C retained only 88% of the capacity of the cell cycled at 25°C after 150 cycles. This comparison indicates that the cell in the string therefore faded at a similar rate at 60°C as that of the cell aged independently. It should be noted that before aging $_{sc}$sf was 1.018 in Cell #2, which was likely due to the fact that the cell was discharged at 60°C and exhibited a higher capacity than those at 25°C. As shown in our prior work,[11] the cell capacity is a function of temperature. As temperature increases, the capacity should be enhanced. Using the capacity at 25°C as the basis, the capacity at 60°C should give a higher $_{sc}$sf, in proportion with the higher temperature.

The $_{sci}$tfs varied from 1.20 and –0.03 to 17.10 and –2.65 after 150 cycles for Cell #2 and #3, respectively. This implies that even though Cell #1 and #3 (both at 25°C) faded the same way (as indicated by the same $_{sc}$sf), the SOC scale in Cell #3 was slightly drifted apart by –2.65% from that of Cell #1 by cycle aging. The SOC scale in Cell #2 was drifted by 17.1% from that of Cell #1, which in turn reduced the pack capacity significantly. These SOC scale changes explained why the pack capacity faded much faster than those of the single cells.

The evolutions of tf and sf at various SOHs were found to evolve linearly with cycle aging. This evolution is indicative of cell imbalance in the string, largely due to the accelerated capacity fade in Cell #2 at 60°C. This observation explains the accelerated linear fade of the capacity in the string. This also suggests that there is no additional fade in the single cells that might come from the string configuration-induced complication as a result of cell imbalance. This ability to track and quantify the evolution of tf and sf with aging allows the prediction of the RUL of the cell assembly based on single cells' RUL via the tracking of the evolution of the cell imbalance.

Conclusions

In this study we explained a unique and simple SOC estimation method in a cell assembly and validated that this approach could reduce the complexity in the SOC determination and track the capacity-based SOH for a battery pack. As we have illustrated in our prior work, the best way to determine the SOC for a battery pack is to use the $OPV = f(_{pack}SOC)$ function, which is hampered by the fact that such a function is not universal for a battery design due to cell variability and pack configuration. Here, we showed that the $OPV = f(_{pack}SOC)$ function could be derived from the $_{SCi}OCV = f(_{SCi}SOC)$ functions in the single cells accurately, accommodating cell variability and pack configuration. This approach simplifies complicated SOC determination in a pack by considering the cell variability and imbalance in the pack, rescaling SOC in each cells of a pack using capacity ration, and calibrating and unifying the SOC scale to become independent of cell variability and imbalance. This approach requires only two measurements of rest cell voltages of all single cells in the pack and the rest pack voltage at two distinct occasions in an aging process. As validated here, the method could track the pack SOC variation with great accuracy. It offers significant benefits to battery control and management. The method does not require intensive computation or complicated calibration and can be easily implemented in a BMS. Additionally, two parameters, tf and sf, were introduced to characterize and track cell imbalance evolution in a pack, thus enabling RUL determination with improved accuracy.

Coupled with other diagnostic tools we have reported previously, we trust that this approach leads to a significant improvement of the quality of BMS SOC tracking and SOH prognosis for applications where large battery assemblies are needed. To the best of our knowledge, this is the first time the pack-level (imbalance) and cell-level (aging) degradation factors in a battery pack could be distinguished and accurately quantified without complicated protocols and procedures. Furthermore, this technique does not need to perform any calibration, physical disassembly, or pack maintenance; thus, it could reduce downtime and loss of efficiency and function.

References

1. L. Lu, X. Han, J. Li, J. Hua, and M. Ouyang, *J. Power Sources*, **226**, 272 (2013).
2. M. U. Cuma and T. Koroglu, *Renewable and Sustainable Energy Reviews*, **42**, 517 (2015).
3. M. Dubarry, N. Vuillaume, and B. Y. Liaw, *Int. J. Energ. Res.*, **34**, 216 (2010).
4. M. Dubarry, N. Vuillaume, and B. Y. Liaw, *J. Power Sources*, **186**, 500 (2009).
5. M. Dubarry, C. Truchot, and B. Y. Liaw, *J. Power Sources*, **219**, 204 (2012).
6. K. L. Gering, S. V. Sazhin, D. K. Jamison, C. J. Michelbacher, B. Y. Liaw, M. Dubarry, and M. Cugnet, *J. Power Sources*, **196**, 3395 (2011).
7. M. Dubarry, C. Truchot, B. Y. Liaw, K. Gering, S. Sazhin, D. Jamison, and C. Michelbacher, *J. Power Sources*, **196**, 10336 (2011).
8. M. Dubarry, C. Truchot, M. Cugnet, B. Y. Liaw, K. Gering, S. Sazhin, D. Jamison, and C. Michelbacher, *J. Power Sources*, **196**, 10328 (2011).
9. M. Dubarry, B. Y. Liaw, M.-S. Chen, S.-S. Chyan, K.-C. Han, W.-T. Sie, and S.-H. Wu, *J. Power Sources*, **196**, 3420 (2011).
10. M. Dubarry and B. Y. Liaw, *J. Power Sources*, **194**, 541 (2009).
11. M. Dubarry, C. Truchot, B. Y. Liaw, K. Gering, S. Sazhin, D. Jamison, and C. Michelbacher, *J. Electrochem. Soc.*, **160**, A191 (2013).
12. C. Truchot, M. Dubarry, and B. Y. Liaw, *Appl. Energy*, **119**, 218 (2014).
13. H. Dai, X. Wei, Z. Sun, J. Wang, and W. Gu, *Appl. Energy*, **95**, 227 (2012).
14. H. He, R. Xiong, and H. Guo, *Appl. Energy*, **89**, 413 (2012).
15. J. Wang, B. Cao, Q. Chen, and F. Wang, *Control Engineering Practice*, **15**, 1569 (2007).
16. L. Zhong, C. Zhang, Y. He, and Z. Chen, *Appl. Energy*, **113**, 558 (2014).
17. F. Sun and R. Xiong, *J. Power Sources*, **274**, 582 (2015).
18. https://www.soest.hawaii.edu/HNEI/alawa/.
19. M. Kassem and C. Delacourt, *J. Power Sources*, **235**, 159 (2013).
20. J. P. Schmidt, H. Y. Tran, J. Richter, E. Ivers-Tiffée, and M. Wohlfahrt-Mehrens, *J. Power Sources*, **239**(1), 696 (2013).
21. M. Kassem, J. Bernard, R. Revel, S. Pélissier, F. Duclaud, and C. Delacourt, *J. Power Sources*, **208**, 296 (2012).
22. M. Dubarry, A. Devie, C. Truchot, and B. Y. Liaw, in preparation.
23. M. Dubarry, A. Devie, C. Truchot, B. Lochner, E. Wong, and B. Y. Liaw, *J. Power Sources*, in preparation (2015).
24. A. Devie, M. Dubarry, and B. Y. Liaw, Abstract A1-0156, the 225th ECS meeting, May 11, Orlando, FL, 2014.